Thermodynamic analysis of group III nitrides grown by metal-organic vapour-phase epitaxy (MOVPE), hydride (or halide) vapour-phase epitaxy (HVPE) and molecular beam epitaxy (MBE)

2001 J. Phys.: Condens. Matter 13 6907

(http://iopscience.iop.org/0953-8984/13/32/303)

INSTITUTE OF PHYSICS PUBLISHING JOURNAL OF PHYSICS: CONDENSED MATTER

J. Phys.: Condens. Matter **13** (2001) 6907–6934 PII: S0953-8984(01)25167-4

Thermodynamic analysis of group III nitrides grown by metal–organic vapour-phase epitaxy (MOVPE), hydride (or halide) vapour-phase epitaxy (HVPE) and molecular beam epitaxy (MBE)

Akinori Koukitu and Yoshinao Kumagai

Department of Applied Chemistry, Faculty of Technology,
Tokyo University of Agriculture and Technology, Koganei, Tokyo 184-8588, Japan

Received 24 May 2001
Published 26 July 2001
Online at stacks.iop.org/JPhysCM/13/6907

Abstract

An analysis of element incorporation from a thermodynamic viewpoint is described for the vapour-phase epitaxy (metal–organic vapour-phase epitaxy (MOVPE), hydride (or halide) vapour-phase epitaxy (HVPE) and molecular beam epitaxy (MBE)) of group III nitrides. The driving force of binary nitrides and the vapour–solid distribution relationship for ternary and quaternary nitrides are discussed. It is shown that the growth rate and alloy composition of group III nitrides are thermodynamically controlled. The thermodynamically predicted orders in which binary nitrides incorporate into alloys are very similar for all epitaxial methods and the order is basically governed by the Gibbs free energy of formation of the binary nitrides irrespective of the growth method.

1. Introduction

Knowledge of the mechanisms that determine the growth rate and the incorporation of elements in vapour-phase epitaxy is important for the growth of compound semiconductors. It provides us with information on suitable growth conditions for the preparation of compound semiconductors, as well as insight into the crystal growth mechanism. If one wishes to understand any vapour growth process, thermodynamics provides very useful information [1–10]. In previous papers [1, 3–10], we showed that an equilibrium model is useful for predicting the growth rate and the element incorporation of III–V compound semiconductors grown by metal–organic vapour-phase epitaxy (MOVPE), hydride (or halide) vapour-phase epitaxy (HVPE) and molecular beam epitaxy (MBE).

Group III nitrides and their alloys have received much attention as materials for use in short-wavelength optical devices and high-temperature electrical devices. Recently, the electrical and optical properties of these materials have been dramatically improved due to the development of growth methods. Epitaxial films of III nitrides can be grown by MOVPE,

HVPE and MBE. It is of interest to investigate the role of growth conditions such as the growth temperature, the input precursor pressure and the total pressure in III nitride growth, because it provides a deeper understanding of the underlying chemistry in the growth of nitrides. The purpose of this paper is to report a thermodynamic analysis of III nitrides grown by MOVPE, HVPE and MBE. In order to calculate the equilibrium partial pressure, a previously developed computation method [1, 3–10] has been extended to the growth system of III nitrides. It will be shown that the present analysis provides an efficient guide for the MOVPE, HVPE and MBE growth of III nitrides. The implications of the difference in growth method for the vapour–solid distribution relationship will also be discussed. Finally, we will describe a thermodynamic calculation system available on the Web.

2. Metal–organic vapour-phase epitaxy (MOVPE)

It is well known that the growth rate of MOVPE is generally temperature independent and group III mass transport limited under commonly used conditions. In other words, the rate is controlled simply by the arrival rate of the growing species at the vapour–solid interface. Under these conditions, if we obtain supersaturated quantities of elements, the growth rate and composition of III nitride compounds can be predicted under given conditions. In this work, the supersaturated quantities of elements and the driving forces of elements are determined by calculating equilibrium partial pressures at the vapour–solid interface. In the equilibrium model described above, the growth rate is expressed as follows:

$$r = k_g(P^0_{III} - P_{III}) \tag{1}$$

where $P^0_{III} - P_{III}$ indicates the driving force for deposition, k_g is a constant, P^0_{III} is the input partial pressure of the group III element and P_{III} is the equilibrium partial pressure at the vapour–solid interface. The dependence of the growth rate and the composition on growth parameters is found by calculating of the values of $P^0_{III} - P_{III}$, i.e. ΔP.

The calculation procedure is shown here for InGaN alloy, to give an example for the MOVPE growth of group III nitrides. The following six species are chosen as the necessary vapour species in analysing the MOVPE growth of $In_xGa_{1-x}N$: In, Ga, NH_3, H_2, RH (CH_4 or C_2H_6) and inert gas (IG). The input metal–organic precursors of In and Ga are decomposed irreversibly, according to the following homogeneous reactions near the vapour–solid interface:

$$R_3In\ (g) + (3/2)H_2\ (g) \rightarrow In\ (g) + 3RH\ (g) \tag{2}$$

$$R_3Ga\ (g) + (3/2)H_2\ (g) \rightarrow Ga\ (g) + 3RH\ (g) \tag{3}$$

The chemical reactions which occur at the substrate surface to form InGaN alloy are

$$In\ (g) + NH_3\ (g) = InN\ (alloy) + (3/2)H_2\ (g) \tag{4}$$

$$Ga\ (g) + NH_3\ (g) = GaN\ (alloy) + (3/2)H_2\ (g) \tag{5}$$

where InN (alloy) and GaN (alloy) stand for the binary compounds in the $In_xGa_{1-x}N$ alloy. Thus the equilibrium equations for these reactions are

$$K_4 = \frac{a_{InN} P^{3/2}_{H_2}}{P_{In} P_{NH_3}} \tag{6}$$

$$K_5 = \frac{a_{GaN} P^{3/2}_{H_2}}{P_{Ga} P_{NH_3}} \tag{7}$$

where a_{InN} and a_{GaN} are the activities of the binary compounds in the alloy. The total pressure of the system is expressed as

$$\sum P_i = P_{In} + P_{Ga} + P_{NH_3} + P_{H_2} + P_{RH} + P_{IG}. \tag{8}$$

From conservation constraints we have

$$P^0_{\mathrm{III}} - P_{\mathrm{III}} = P^0_{\mathrm{V}} - P_{\mathrm{V}} \tag{9}$$

$$P_{\mathrm{RH}} = 3P^0_{\mathrm{III}} \tag{10}$$

where P^0_{III} and P^0_{V} are the input partial pressures of group III and group V species. Equation (9) indicates that deposition occurs in the ratio of 1 to 1 for group III and group V elements. The mole fraction x in the $\mathrm{In}_x\mathrm{Ga}_{1-x}\mathrm{N}$ alloy is given by

$$x = \frac{P^0_{\mathrm{In}} - P_{\mathrm{In}}}{(P^0_{\mathrm{In}} - P_{\mathrm{In}}) + (P^0_{\mathrm{Ga}} - P_{\mathrm{Ga}})}. \tag{11}$$

In addition, the parameters F and α are introduced:

$$F = \frac{P^0_{\mathrm{H_2}}}{P^0_{\mathrm{H_2}} + P^0_{\mathrm{IG}}}. \tag{12}$$

F is the mole fraction of H_2 relative to the inert gas, such as nitrogen in the carrier gas, where $P^0_{\mathrm{H_2}}$ and P^0_{IG} indicate the input partial pressures of H_2 and IG. Under complete equilibrium conditions, most of the NH_3 is expected to decompose into N_2 and H_2 at temperatures higher than 300 °C. However, it is well known that the rate of decomposition of NH_3 under typical growth conditions is slow without a catalyst and the extent of the decomposition strongly depends on the growth conditions and growing equipment [11–13]. Therefore, we introduced α in the calculation as follows:

$$\mathrm{NH_3\ (g)} \rightarrow (1-\alpha)\mathrm{NH_3\ (g)} + (1/2)\alpha\mathrm{N_2\ (g)} + (3/2)\alpha\mathrm{H_2\ (g)}. \tag{13}$$

The equilibrium partial pressures and the vapour–solid distribution relationship were calculated by using a method similar to that developed previously [3, 4, 6, 7]. The values of the equilibrium constants are listed in table 1. The activities in the alloy were calculated using the delta lattice parameter (DLP) model [14].

Table 1. Equilibrium constants [7, 9, 35–37].

Methods	Reactions	$\log_{10}(K\ (\mathrm{K}))$
MOVPE, GSMBE	$\mathrm{Ga\ (g) + NH_3\ (g) = GaN\ (s) + (3/2)H_2\ (g)}$	$12.2 + 1.78 \times 10^4/T + 1.79\log_{10}(T)$
	$\mathrm{In\ (g) + NH_3\ (g) = InN\ (s) + (3/2)H_2\ (g)}$	$13.1 + 1.13 \times 10^4/T + 2.29\log_{10}(T)$
	$\mathrm{Al\ (g) + NH_3\ (g) = AlN\ (s) + (3/2)H_2\ (g)}$	$14.2 + 3.17 \times 10^4/T + 2.33\log_{10}(T)$
MBE	$\mathrm{Ga\ (g) + N\ (g) = GaN\ (s)}$	$16.0 + 4.48 \times 10^4/T + 0.147\log_{10}(T)$
	$\mathrm{In\ (g) + N\ (g) = InN\ (s)}$	$15.7 + 3.82 \times 10^4/T + 0.289\log_{10}(T)$
	$\mathrm{Al\ (g) + N\ (g) = AlN\ (s)}$	$17.7 + 5.44 \times 10^4/T + 0.661\log_{10}(T)$
HVPE	$\mathrm{GaCl\ (g) + NH_3\ (g) = GaN\ (s) + HCl\ (g) + H_2\ (g)}$	$9.08 + 4.04 \times 10^3/T + 1.72\log_{10}(T)$
	$\mathrm{InCl\ (g) + NH_3\ (g) = InN\ (s) + HCl\ (g) + H_2\ (g)}$	$10.3 - 4.30 \times 10^2/T + 2.20\log_{10}(T)$
	$\mathrm{AlCl\ (g) + NH_3\ (g) = AlN\ (s) + HCl\ (g) + H_2\ (g)}$	$10.4 + 1.68 \times 10^4/T + 2.11\log_{10}(T)$
THVPE	$\mathrm{GaCl_3\ (g) + NH_3\ (g) = GaN\ (s) + 3HCl\ (g)}$	$2.82 - 5.61 \times 10^3/T + 0.430\log_{10}(T)$
	$\mathrm{InCl_3\ (g) + NH_3\ (g) = InN\ (s) + 3HCl\ (g)}$	$1.14 - 6.46 \times 10^3/T + 0.931\log_{10}(T)$
	$\mathrm{AlCl_3\ (g) + NH_3\ (g) = AlN\ (s) + 3HCl\ (g)}$	$2.14 - 1.77 \times 10^3/T + 0.628\log_{10}(T)$

2.1. Binary group III nitrides

Figures 1 to 3 show the equilibrium partial pressures over GaN, InN and AlN in MOVPE as functions of the input V/III ratio. The dashed lines in the figures indicate the partial pressures

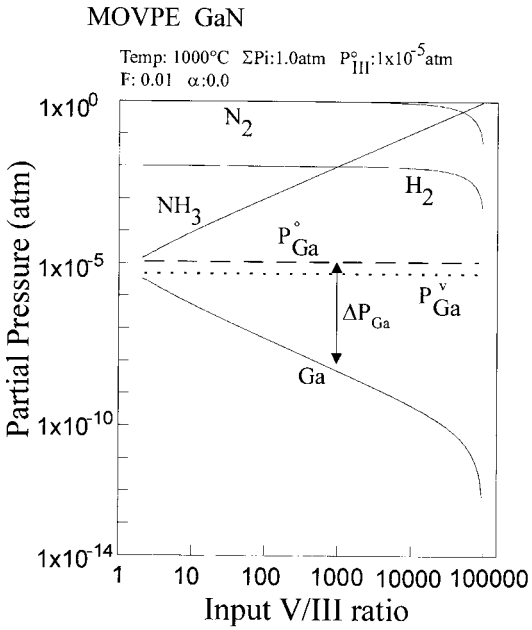

Figure 1. The equilibrium partial pressures as functions of the input V/III ratio. Dashed and dotted lines indicate the input partial pressure of Ga and the vapour pressure of metallic Ga, respectively.

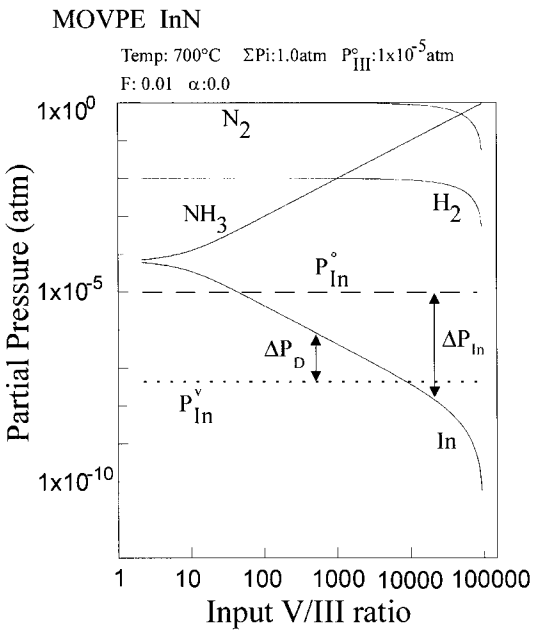

Figure 2. The equilibrium partial pressures as functions of the input V/III ratio. Dashed and dotted lines indicate the input partial pressure of In and the vapour pressure of metallic In, respectively.

of the input group III species ($P^0_{\rm III}$) and the dotted lines show the vapour pressures of the group III metal ($P^{\rm v}_{\rm III}$). The general features of the equilibrium partial pressures are similar to those

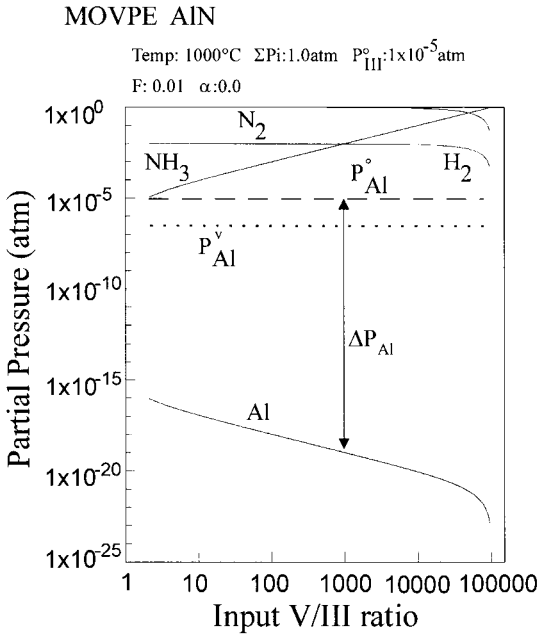

Figure 3. The equilibrium partial pressures as functions of the input V/III ratio. Dashed and dotted lines indicate the input partial pressure of Al and the vapour pressure of metallic Al, respectively.

of the other III–V compounds in MOVPE growth [3, 4, 15]. The equilibrium partial pressures of the group III elements are sensitive to the input V/III ratio, as seen in figures 1 to 3. In particular, for a low V/III ratio, the pressures of Ga and In remain high in the vapour phase in contrast to the case for other III–V compounds [3, 4, 15] in which the partial pressures of the group III species are generally lower than 1×10^{-8} atm. Therefore, the driving force for the deposition ($\Delta P_{\mathrm{III}} = P^0_{\mathrm{III}} - P_{\mathrm{III}}$) decreases with decrease of the input V/III ratio.

One of the important features in figure 2 is that there exist three deposition modes in InN growth corresponding to the input V/III ratio. At low input ratio (V/III $<$ 40), etching of InN may occur, because the equilibrium partial pressure of In, P_{In}, is higher than P^0_{III}. In the middle region (40 $<$ V/III $<$ 10 000), we may have indium droplets (ΔP_{D}) on the growing surface, because P_{In} is higher than $P^{\mathrm{v}}_{\mathrm{In}}$ but lower than P^0_{In}. Therefore, higher input V/III ratios (V/III $>$ 10 000) are required for the deposition of InN.

Figure 4 shows the phase diagram of the deposition calculated for GaN, InN and AlN, showing the three deposition modes displayed in figure 2 versus the input P^0_{III} and V/III ratio. There are three deposition modes: etching ($P_{\mathrm{III}} > P^0_{\mathrm{III}}$), droplet ($P_{\mathrm{III}} > P^{\mathrm{v}}_{\mathrm{III}}$) and growth ($P_{\mathrm{III}} < P^0_{\mathrm{III}}$ and $P_{\mathrm{III}} < P^{\mathrm{v}}_{\mathrm{III}}$) regions. The greyscale in the growth region indicates the magnitude of the driving force, ΔP_{III}. In the figure, the total pressure ($\sum P_i$), H_2 mole fraction in the carrier gas (F) and mole fraction of decomposed NH_3 (α) are kept constant at 1.0 atm, 0.01 and 0.0, respectively. It is seen that the deposition of GaN is possible over a wide range of conditions at 800 °C, and the region of etching increases with increasing growth temperature. The growth rate in the growth region is predicted to increase with the increase of the input P^0_{III} at a constant V/III ratio. Furthermore, AlN can be grown under all conditions at temperatures between 800 and 1200 °C. In contrast to the case for GaN and AlN, the regions suitable for deposition of InN are very narrow. The droplet mode is dominant in deposition at low temperature, while at high temperatures, the etching mode becomes dominant. Figure 4

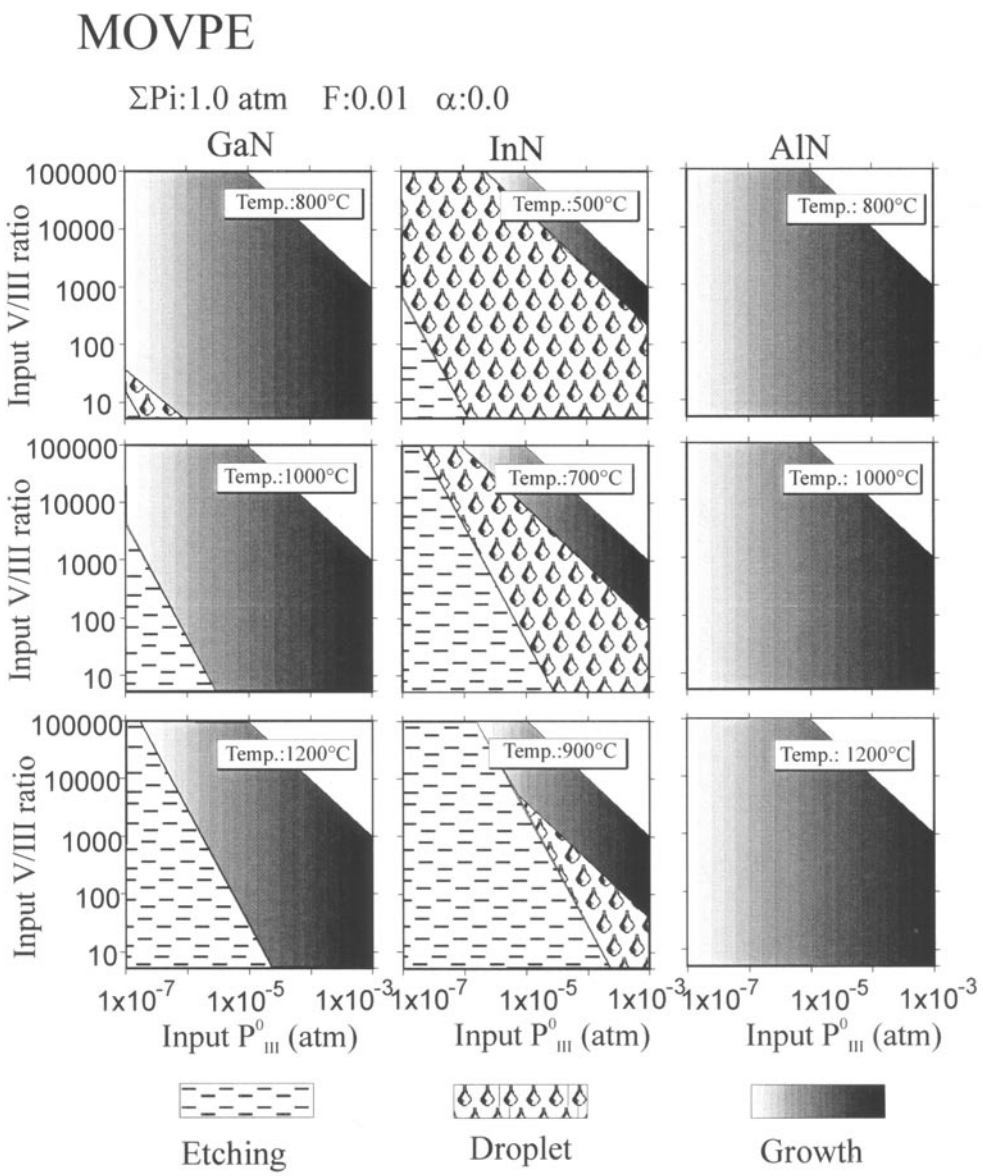

Figure 4. The calculated phase diagrams for the deposition of GaN, InN and AlN versus the input P^0_{III} and V/III ratio. The values of $\sum P_i$, F and α are kept constant at 1.0 atm, 0.01 and 0.0, respectively. There are three deposition modes: etching, droplets and growth.

indicates that a high input NH_3 pressure is required to grow InN, because the NH_3 pressure is expressed by $P^0_{\mathrm{III}} \times \mathrm{V/III}$ ratio.

From the results, the order of deposition of nitrides is

$$\mathrm{AlN} > \mathrm{GaN} \gg \mathrm{InN}. \tag{14}$$

This order agrees with the order of the equilibrium constants of the formation reaction of the binary nitride compounds, III (g) + $(3/2)NH_3$ (g) $\rightarrow$ III–N (s) + $(3/2)H_2$ (g). In the growth of ternary and quaternary alloys such as AlGaN, InGaN and InGaAlN, it will be shown that

the solid composition of the group III elements is governed by that order, as will be shown later in sections 2.2 and 2.3.

2.2. Ternary group III nitrides

Figures 5 to 7 show the equilibrium partial pressures of gaseous species over $In_xGa_{1-x}N$ alloys. The dotted lines show the vapour pressures of metallic In and Ga, P^v_{In} and P^v_{Ga}. The general features of the equilibrium partial pressures are similar to those of GaN and InN in the MOVPE growth as shown in figures 1 and 2. The equilibrium partial pressures of Ga and In change widely with the input V/III ratio and mole fraction of decomposed NH_3, while their changes are small for the solid composition. One important feature in these figures is that the equilibrium partial pressure of In is significantly higher than that of Ga. This is due to the fact that the equilibrium constant of equation (4) is smaller than that of equation (5), and this fact causes the deviation of the solid composition from the linear function of the input mole ratio which will be described later.

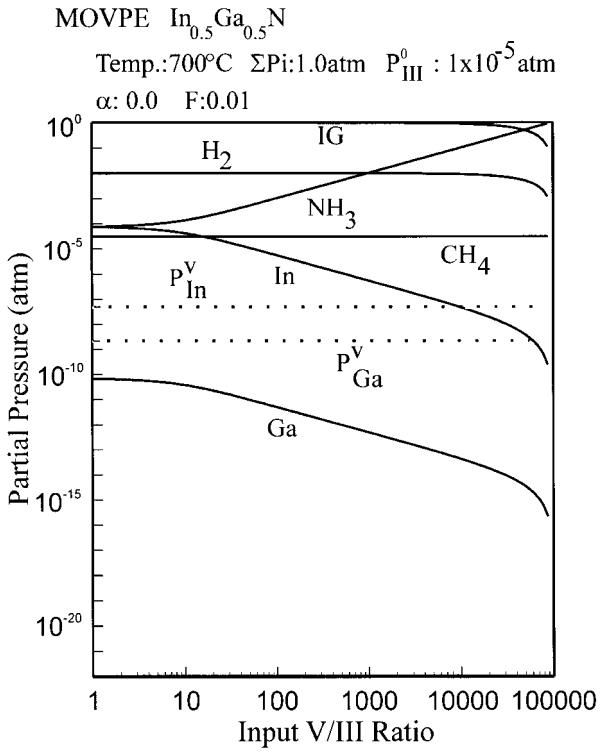

Figure 5. The equilibrium pressures over $In_{0.5}Ga_{0.5}N$ as functions of the input V/III ratio at 700 °C. The dotted lines indicate the vapour pressure of metallic Ga and In.

Another important feature is that we may have indium droplets on the growing surface, because there are regions where P_{In} is higher than P^v_{In}. Similarly, we may have etching, because there are regions where P_{III} is higher than P^0_{III}. Therefore, in the $In_xGa_{1-x}N$ growth, there exist three deposition modes: the growth region ($P_{III} < P^0_{III}$ and $P_{III} < P^v_{III}$), indium droplets ($P_{III} > P^v_{III}$) and etching ($P_{III} > P^0_{III}$). These results indicate that a high V/III ratio is required to obtain a suitable deposition of InGaN preventing indium droplet deposition.

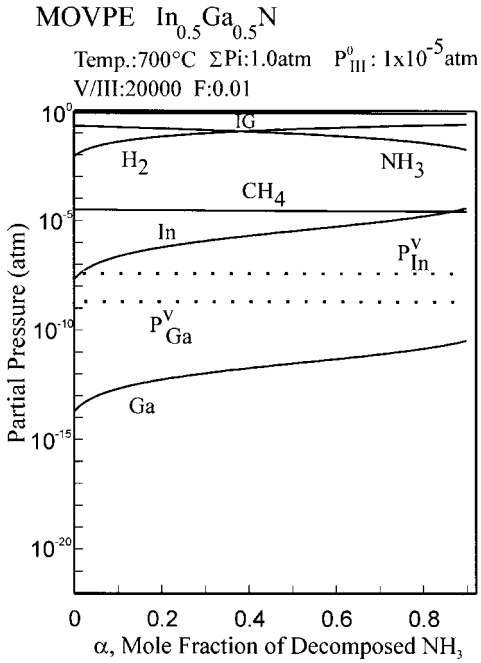

Figure 6. The equilibrium pressures over $In_{0.5}Ga_{0.5}N$ as functions of the parameter α, which is the mole fraction of decomposed NH_3. The dotted lines indicate the vapour pressure of metallic Ga and In.

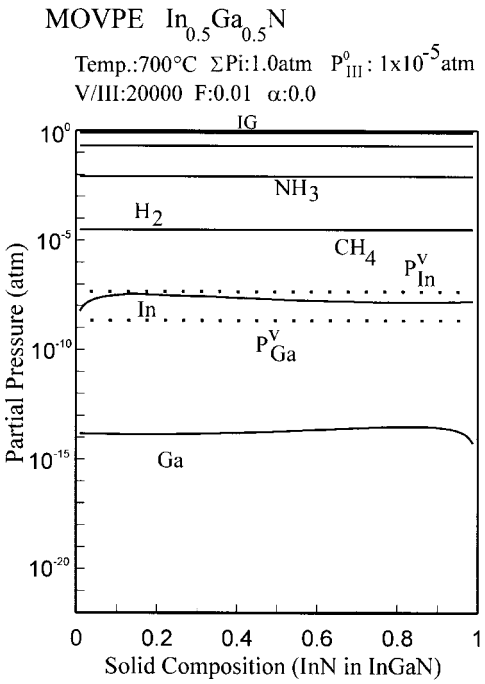

Figure 7. The equilibrium pressures as functions of the solid composition, x, in the $In_xGa_{1-x}N$ alloy. The dotted lines indicate the vapour pressure of metallic Ga and In.

Figures 8 to 10 show theoretical curves of the $In_xGa_{1-x}N$ solid composition as functions of the input mole ratio of the group III metal–organic sources calculated for several values of α, input V/III ratio and growth temperature. It is seen that the solid composition strongly depends on these parameters with similar behaviours. For example, in figure 8, the solid composition is a linear function of the input ratio at $\alpha = 0.0$. However, with the increase of α, the solid composition deviates from the linear function and the indium content in the solid becomes about 0.1 for the input mole ratio of 0.7 at $\alpha = 0.2$. A similar deviation occurs with the increase of the parameter F. These facts suggest that hydrogen in the growth system plays an important role in the deviation of the alloy composition. On the other hand, the effect of the input V/III ratio on the deviation is rather small at the commonly used high input V/III ratio, as seen in figure 9. Also, the effect of the growth temperature is small at low temperature, but a large deviation occurs at high temperature.

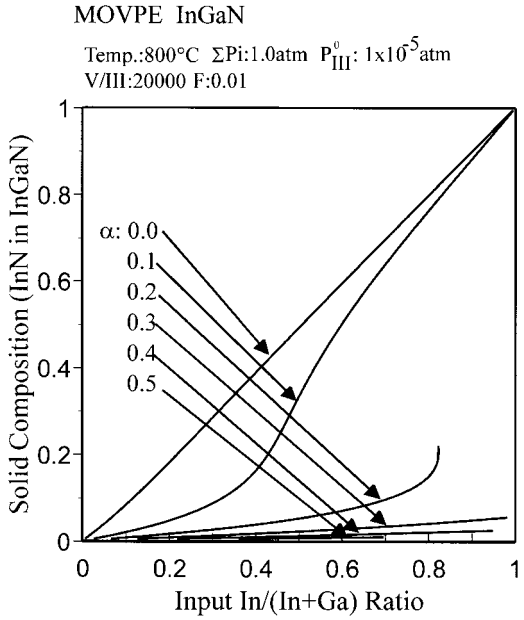

Figure 8. Theoretical curves of the $In_xGa_{1-x}N$ solid composition as a function of the input ratio of the group III metal–organic sources at 800 °C, varying the value of α.

In figure 11, the theoretically predicted compositions of $In_xGa_{1-x}N$ alloys are compared with the experimental data reported by Matsuoka *et al* [16]. The value of α in the calculation was determined as a fitting parameter, because it is difficult to know the exact value. At the growth temperature of 500 °C, the solid composition of $In_xGa_{1-x}N$ is independent of α. The agreement between the experimental and calculated compositions is quite good, which shows that the solid composition of $In_xGa_{1-x}N$ alloy growth by MOVPE is thermodynamically controlled.

As described in previous papers [3, 4, 15], the equilibrium partial pressures of the group III elements over alloys of the column III phosphides, arsenides and antimonides are very low compared with the input partial pressures when the V/III ratio is larger than unity. Consequently, the mole fraction, x, in the $III_xIII'_{1-x}V$ alloy is

$$x = \frac{P^0_{III} - P_{III}}{(P^0_{III} - P_{III}) + (P^0_{III'} - P_{III'})} \simeq \frac{P^0_{III}}{(P^0_{III} - P_{III'})} \tag{15}$$

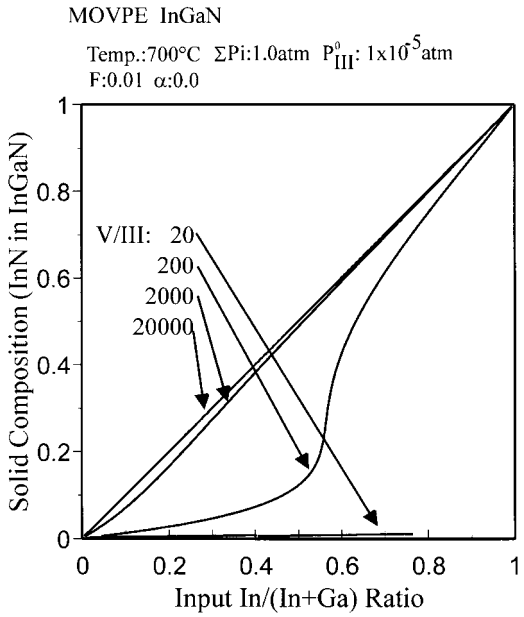

Figure 9. Theoretical curves of the $In_xGa_{1-x}N$ solid composition as a function of the input ratio of the group III metal–organic sources at 700 °C, varying the input V/III ratio.

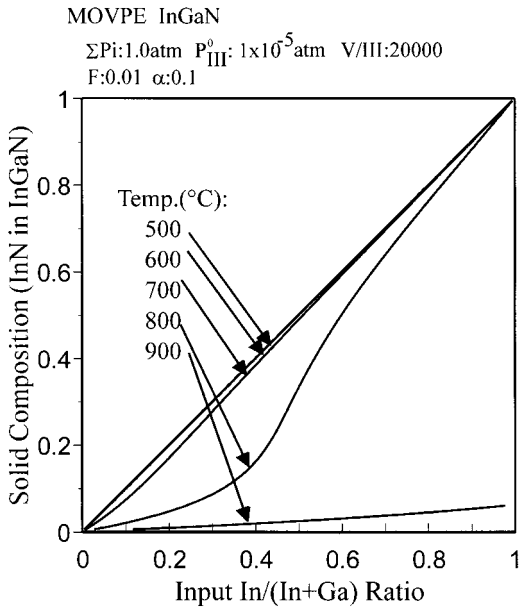

Figure 10. Theoretical curves of the $In_xGa_{1-x}N$ solid composition as a function of the input ratio of the group III metal–organic sources, varying the temperature.

where P^0_{III} and $P^0_{III'}$ are the input partial pressures and P_{III} and $P_{III'}$ are the equilibrium partial pressures. Therefore, the incorporation of group III elements into the solid phase becomes a linear function of the input mole ratio of the group III metal–organic sources under typical

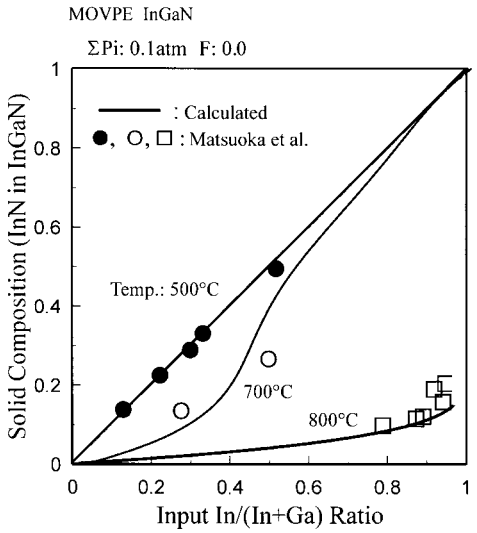

Figure 11. Comparison between the theoretically predicted and experimental compositions of $In_xGa_{1-x}N$ alloys at 500, 700 and 800 °C. The calculation conditions were the same as those used by Matsuoka *et al*, i.e. the input partial pressures, V/III ratios and α were: 3×10^{-6} atm, 20 000 and 0.0 at 500 °C; 3.6×10^{-6} atm, 25 000 and 2.5 at 700 °C; and 1×10^{-5} atm, 5000 and 0.35 at 800 °C.

growth conditions. In $In_xGa_{1-x}N$ alloys, this rule holds under conditions of low value of α, high input V/III ratio and low temperature, as seen in figures 8 to 10. However, under conditions of high value of α, low input V/III ratio and high temperature, the equilibrium partial pressure of In becomes of an order comparable to that of the input partial pressure. As a result, the solid composition deviates from the linear function.

At high temperature, H_2 is produced by the decomposition of NH_3. Also, we can increase H_2 by changing F. The increase of H_2 in these ways drives equation (4) to the left. This causes the deviation of the solid composition from the linear relation, because the equilibrium partial pressure of In increases to a high value. Consequently, hydrogen in the growth system plays an important role in the incorporation of In. The composition deviation from the linear relation is attributable to the high equilibrium partial pressure of In.

In ternary alloys such as InGaN, AlGaN and InAlN, achieving epitaxial growth of InAlN is very difficult as predicted from the results described above. To develop the investigation, it is necessary to find favourable growth conditions for the deposition of high-quality InAlN. Figure 12 shows the equilibrium partial pressures of gaseous species over $In_xAl_{1-x}N$ alloys. The dashed line shows the input partial pressure of group III species, P^0_{III}. One important feature in this figure is that the equilibrium partial pressure of In is significantly higher than that of Al. This is due to the fact that the equilibrium constant of the reaction for the InN formation shown in equation (4) is significantly smaller than that of the AlN formation. Another important feature is that we can obtain $In_xAl_{1-x}N$ with any solid composition between $x = 0$ and $x = 1$, because P_{III} is smaller than P^0_{III} over the whole range of solid composition at 700 °C.

Figure 13 shows the theoretical curves of the $In_xAl_{1-x}N$ solid composition as a function of the input mole ratio of the group III metal–organic sources for several growth temperatures. In the calculation, the condition of almost inert carrier gas ($F = 0.01$) is selected, and the values of α are determined by reference to that for InGaN given above. At low temperature, the solid composition is a linear function of the input mole ratio of the group III metal–organic

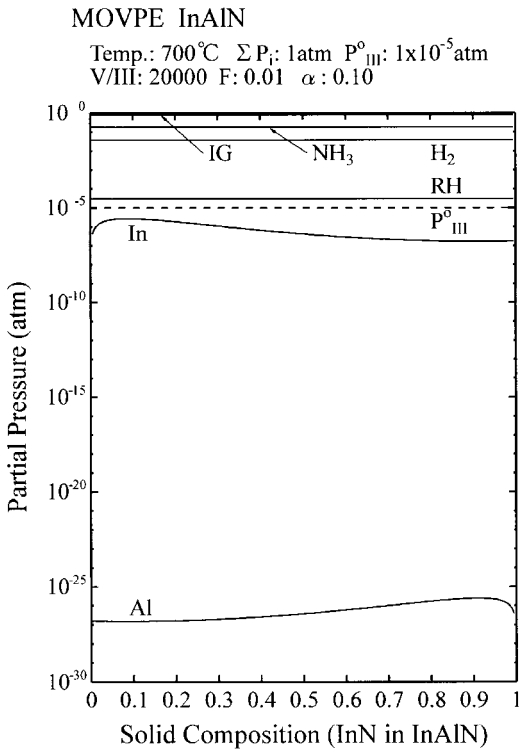

Figure 12. Equilibrium partial pressures over $In_xAl_{1-x}N$ as functions of the solid composition (x) at 700 °C. The dashed line indicates the input partial pressure of the group III species.

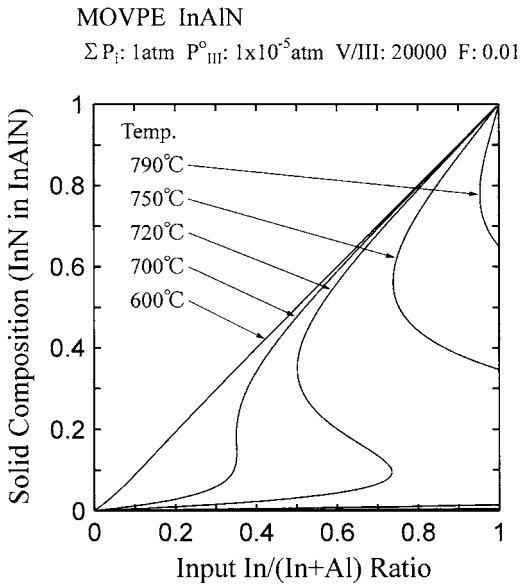

Figure 13. Theoretical curves showing $In_xAl_{1-x}N$ solid composition as a function of the input mole ratio of the group III metal–organic sources. α is 0.05 at 600 °C, 0.10 at 700 °C, 0.15 at 720 °C, 0.25 at 750 °C and 0.30 at 790 °C.

sources. With the increase of the growth temperature, however, the solid composition deviates significantly from the linear relation. At 790 °C, it is very difficult to grow $In_xAl_{1-x}N$, because etching occurs under most growth conditions. One important feature in this figure is that isotemperature lines change in a complex manner at high temperature. This indicates that the deposition of compounds with various solid compositions is expected for a given input mole ratio of the group III metal–organic sources. That is, it is shown that the unstable regions in which inhomogeneous compositions are formed for a given input mole ratio exist in the InAlN alloy system, as described later.

In the case of AlGaN, the solid composition is a linear function of the input mole ratio of the group III sources under typical growth conditions. This is due to the fact that the equilibrium constants of the formation reactions for AlN and GaN are large and the equilibrium partial pressures of the group III elements are significantly smaller compared with the input partial pressures of the group III elements.

2.3. Quaternary group III nitrides

The thermodynamic analysis of InGaAlN, as an example of a quaternary nitride, is described here. The growth and properties of quaternary nitrides, $In_xGa_yAl_{1-x-y}N$, have not been extensively studied to date due to the difficulties in the determination of optimal growth conditions [17–22]. Figure 14 shows the equilibrium partial pressures over $In_{0.14}Ga_{0.20}Al_{0.66}N$ alloy lattice-matched to GaN as functions of growth temperature. The input mole ratios of the group III sources necessary for growing the alloy at each temperature are also shown in the lower part of the figure, where R_{In}, R_{Ga} and R_{Al} indicate the input mole fraction ratios relative to the total pressure of the input group III sources. As can be seen, the equilibrium partial pressure of In is significantly higher than that of Ga and Al, and increases with increasing growth temperature. One important feature is that P_{In} exceeds the input partial pressure of the group III species shown as a dotted line in the figure at temperatures of more than 780 °C. This fact means that the growth mode above 780 °C is etching, and growth is not expected, whereas growth is possible below 780 °C [10].

3. Hydride vapour-phase epitaxy (HVPE)

Hydride vapour-phase epitaxy (HVPE) was the most successful epitaxial growth method during early investigations of the group III nitrides. Using this method, the first single-crystal GaN thin films were realized [23]. Recently, the high growth rate of HVPE has received much attention as regards its use in preparing thick single crystals of GaN with low dislocation density [24, 25]. Now, we report a thermodynamic analysis on the HVPE of GaN, InN and their ternary alloy. We will demonstrate that the present analysis provides us with information on suitable conditions for the HVPE growth, as well as an insight into the chemistry involved in the epitaxial growth.

The calculation procedure for GaN is shown here, to give an example for the HVPE GaN growth. The following six species were chosen as the necessary vapour species in analysing the vapour growth of GaN: GaCl, $GaCl_3$, NH_3, HCl, H_2 and inert gas (IG). The chemical reactions which connect the species in the deposition zone are

$$GaCl\ (g) + NH_3\ (g) = GaN\ (s) + HCl\ (g) + H_2\ (g) \tag{16}$$

$$GaCl\ (g) + 2HCl\ (g) = GaCl_3\ (g) + H_2\ (g). \tag{17}$$

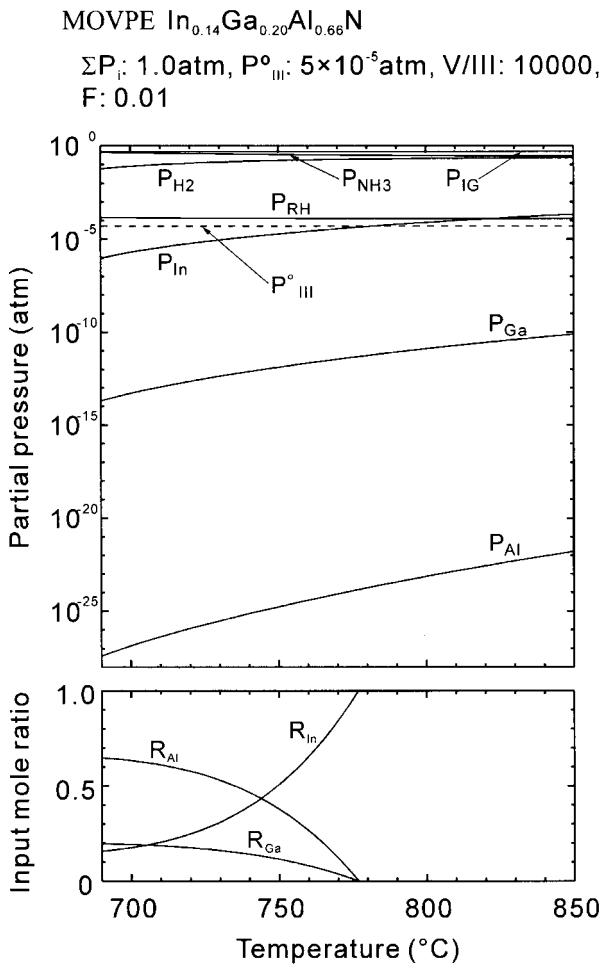

Figure 14. Equilibrium partial pressures over $In_{014}Ga_{0.20}Al_{0.66}N$, a lattice-matched composition for GaN, as functions of growth temperature (upper). The dotted line indicates the input partial pressure of the group III species. Necessary input mole ratios of In (R_{In}), Ga (R_{Ga}) and Al (R_{Al}) for the growth of $In_{014}Ga_{0.20}Al_{0.66}N$ are also shown (lower).

The equilibrium equations for these reactions are

$$K_{16} = \frac{P_{HCl} P_{H_2}}{P_{GaCl} P_{NH_3}} \tag{18}$$

and

$$K_{17} = \frac{P_{GaCl_3} P_{H_2}}{P_{GaCl} P_{HCl}^2}. \tag{19}$$

The values of the equilibrium constants used in the calculation are listed in table 1.

The total pressure of the system can be written as

$$\sum P_i = P_{GaCl} + P_{GaCl_3} + P_{NH_3} + P_{HCl} + P_{H_2} + P_{IG} \tag{20}$$

where the P_i are the equilibrium partial pressures. Denoting the input partial pressures as P_i^0, we have equation (21) from the conservation constraint:

$$P_{GaCl}^0 - P_{GaCl} = P_{NH_3}^0 - P_{NH_3}. \tag{21}$$

This equation shows the stoichiometric relationship for III–V nitride deposition. In addition, the parameters A and F are introduced:

$$A = \frac{(1/2)(P_{GaCl} + 3P_{GaCl_3} + P_{HCl})}{P_{H_2} + (3/2)P_{NH_3} + (1/2)P_{HCl} + P_{IG}} \tag{22}$$

$$F = \frac{(1/2)(2P_{H_2} + 3P_{NH_3} + P_{HCl})}{P_{H_2} + (3/2)P_{NH_3} + (1/2)P_{HCl} + P_{IG}}. \tag{23}$$

A is the ratio of the number of chloride atoms to the number of hydrogen and inert-gas atoms in the system. F is the mole fraction of hydrogen relative to inert-gas atoms. These parameters are kept invariant under a given growth condition, because A does not include any atoms which deposit into a solid. As described for the MOVPE growth, we should introduce a parameter α, the mole fraction of decomposed NH_3, which can be expressed by equation (13). In the following calculation, the change of α affects the change of H_2, N_2 and NH_3 partial pressures in the growth system. A similar result is produced by changing the parameter F. Consequently, we performed the following calculation by changing the parameter F, and fixed α as 0.03, the value according to Ban's experiments in a quartz reactor at 950 °C [26], because it is difficult to know the exact value.

3.1. Binary group III nitrides

Figure 15 shows the equilibrium partial pressures as functions of growth temperature. The general features of the equilibrium partial pressures are similar to those of the hydride systems

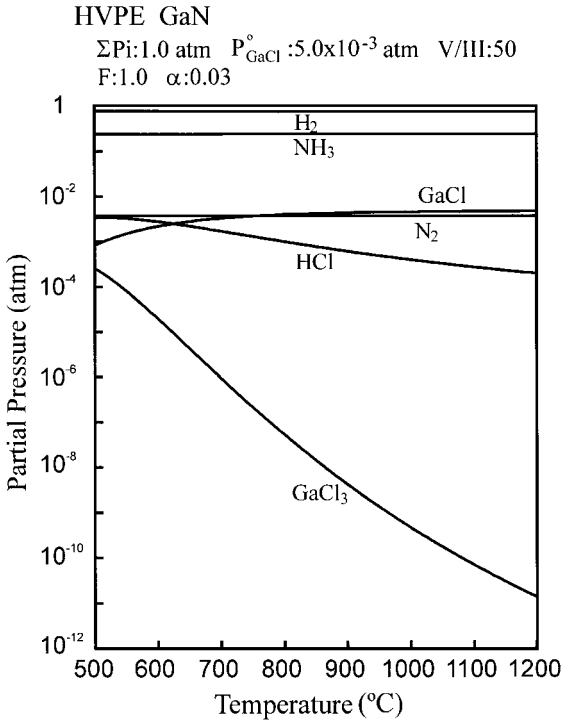

Figure 15. Equilibrium partial pressures over GaN as functions of growth temperature. Total pressure: 1.0 atm; input partial pressure of GaCl: 5×10^{-3} atm; input V/III ratio: 50; F: 1.0; and α: 0.03.

of arsenides and phosphides of Ga and In [27, 28]. It is seen that NH_3, GaCl, N_2 and HCl, but not the hydrogen carrier gas, are major vapour species. Since Ga is transported as GaCl from the source zone and GaN is deposited with HCl, the reaction governing the growth at the substrate may be described as

$$\mathrm{GaCl\ (g) + NH_3\ (g) = GaN\ (s) + HCl\ (g) + H_2\ (g).} \tag{24}$$

In figure 16, ΔP_{Ga} $(=P^0_{\mathrm{GaCl}} - (P_{\mathrm{GaCl}} + P_{\mathrm{GaCl_3}}))$, i.e., the driving force for the deposition, is shown as a function of temperature. The driving force for the deposition decreases with increasing parameter F. Therefore, we can expect a higher growth rate to be obtained in the inert-gas system than in the H_2 system. This agrees well with Ban's experiments [26], where it was shown that the extent of GaCl consumption, i.e., the deposition of GaN, was significantly greater for He as the carrier gas than for H_2.

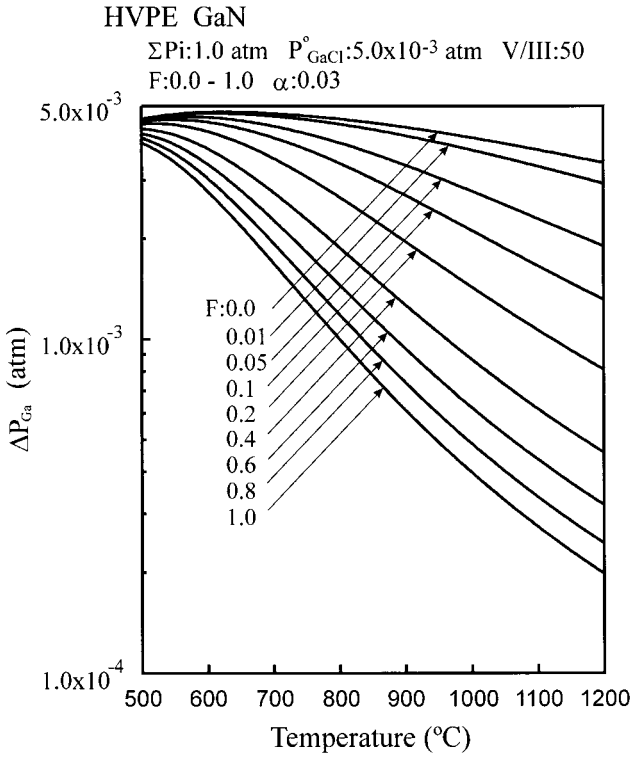

Figure 16. The driving force for the deposition as a function of growth temperature, with various parameters F. Total pressure: 1.0 atm; input partial pressure of GaCl: 5×10^{-3} atm; input V/III ratio: 50; and α: 0.03.

Next, we discuss the HVPE of InN using InCl or $InCl_3$ as the In source. In the previous papers [29, 30], we showed experimentally that vapour-phase epitaxy (VPE) of InN was possible at growth temperatures as high as 750 °C using $InCl_3$ and NH_3, whereas it was difficult to obtain an appreciable growth rate using InCl and NH_3. In order to understand the difference between $InCl_3$ and InCl as regards the deposition of InN and to find suitable growth conditions for InN epitaxial layers, a thermodynamic analysis has been performed for the HVPE of InN using InCl or $InCl_3$. The calculation procedure for the HVPE of InN using InCl and NH_3 is similar to that for the GaN HVPE described above. In the case of

the InN HVPE using $InCl_3$ and NH_3, the following seven species are chosen as the necessary vapour species in analysing this system: $InCl_3$, InCl, NH_3, HCl, H_2, Cl_2 and an inert gas (IG) such as He or N_2. The chemical reactions which connect the species at the vapour–solid interface are

$$InCl_3\ (g) + NH_3\ (g) = InN\ (s) + 3HCl\ (g) \tag{25}$$

$$InCl_3\ (g) = InCl\ (g) + Cl_2\ (g) \tag{26}$$

$$H_2\ (g) + Cl_2\ (g) = 2HCl\ (g). \tag{27}$$

The equilibrium partial pressures were calculated using a method similar to that applied to the GaN HVPE.

Figure 17 shows the driving force for the deposition of InN using InCl (HVPE) or $InCl_3$ (tri-halide vapour-phase epitaxy: THVPE) as the In source. In the InCl system, the driving force is nearly equal to zero both for inert ($F = 0.0$) and hydrogen ($F = 1.0$) carrier gas over the whole temperature range. This indicates that achieving HVPE of InN using InCl is very difficult, and this thermodynamical prediction agrees with our results for the InN HVPE using the InCl source. On the other hand, the driving force strongly depends on the value of F in the $InCl_3$ system (THVPE). If the value of F equals zero, growth of InN is possible over the whole temperature range, whereas the driving force takes a large negative value over the whole temperature range when the value of F equals 1.0. Therefore, the growth of InN via the reaction between $InCl_3$ and NH_3 is possible only with inert carrier gas or a mixed carrier

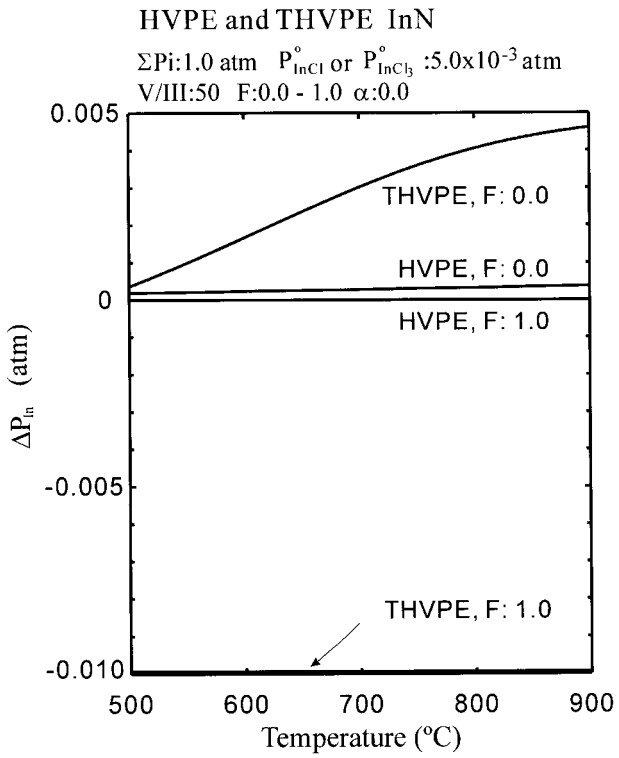

Figure 17. Driving forces for the deposition of InN using InCl (HVPE) or $InCl_3$ (THVPE) as functions of growth temperature. The calculation was performed for the growth under an inert carrier gas ($F = 0.0$) and hydrogen carrier gas ($F = 1.0$).

gas made up of hydrogen and inert gas. These results agree well with the experimental data reported previously [29, 30]. Furthermore, it can be predicted that HVPE growth of InGaN is possible when $InCl_3$ is used as the In source.

3.2. Ternary group III nitrides

Now, we discuss thermodynamic analysis of the THVPE of $In_xGa_{1-x}N$ using $GaCl_3$ and $InCl_3$. The vapour–solid distribution relation of $In_xGa_{1-x}N$ alloy deposition was calculated by comparison with the experimental data. The calculation procedure for this system is similar to that described above. The following nine species were chosen as the necessary vapour species in analysing the THVPE of InGaN: $InCl_3$, InCl, $GaCl_3$, GaCl, NH_3, HCl, Cl_2, H_2 and IG.

Figures 18 and 19 show the vapour–solid distribution relation of InGaN alloy calculated for several values of input V/III ratio and parameter α, respectively. As can be seen in these figures, the solid composition x deviates from a linear function and becomes GaN rich with decrease of the input V/III ratio and with increase of the parameter α; these tendencies are similar to those in the MOVPE of InGaN as shown in figures 8 and 9. In figure 19, due to the large interaction parameter of InGaN alloy, there exist unstable regions with α above 0.05 in which compounds with inhomogeneous compositions are formed for a given input mole ratio of group III sources. From this result, it is evident that the solid composition is affected by the addition of hydrogen in the carrier gas, because the increase of α corresponds to the increase of hydrogen in the carrier gas. This is consistent with the rapid decrease of InN incorporation observed in the experimental data [31].

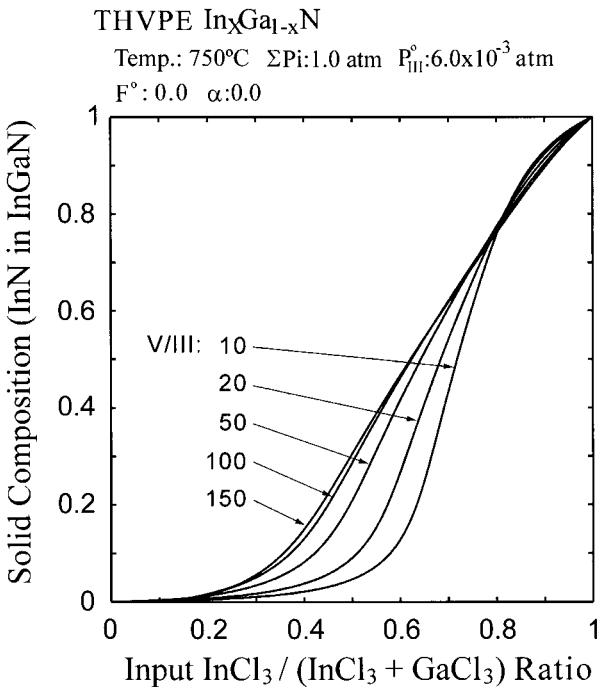

Figure 18. Theoretical curves showing the solid composition of deposited $In_xGa_{1-x}N$ as a function of the input mole ratio of the group III sources at 750 °C, varying the input V/III ratio from 10 to 150.

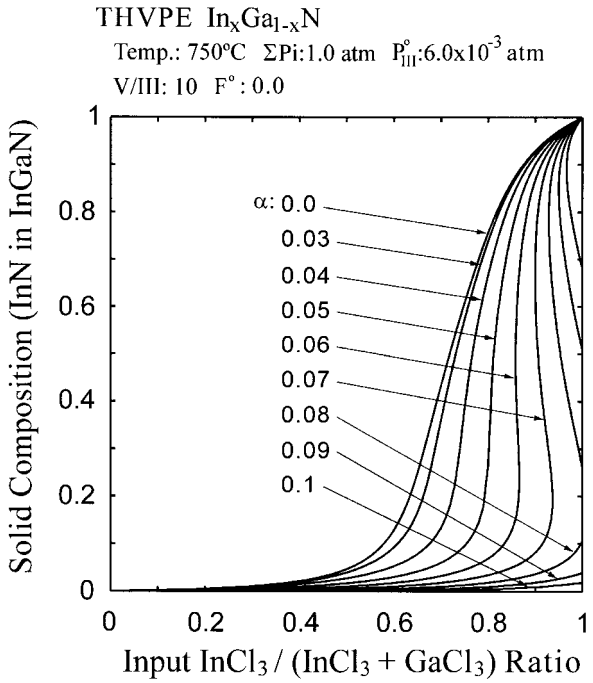

Figure 19. Theoretical curves showing the solid composition of deposited $In_xGa_{1-x}N$ as a function of the input mole ratio of the group III sources at 750 °C, varying the value of α from 0.0 to 0.1.

In figure 20, the theoretically predicted solid composition x in $In_xGa_{1-x}N$ is compared with the experimental data reported by us previously [31]. The value of α in the calculation was determined as a fitting parameter, because it is difficult to know the value for our experimental set-up. The agreement between the experimental and calculated solid compositions is good, showing that the solid composition of InGaN alloys grown using $InCl_3$ and $GaCl_3$ as group III sources is thermodynamically controlled.

4. Molecular beam epitaxy (MBE)

Recently, it has become possible to grow epitaxial films of group III nitrides by MBE as well as by MOVPE and HVPE. To control the MBE process, it is important to know the mechanisms determining the growth rate and alloy composition. If one wishes to understand any vapour growth process, thermodynamics can provide very useful information. In previous work [5, 32], we showed that an equilibrium model is useful for predicting the growth rate and composition for both III–V and II–VI compounds grown by MBE. Here, we extend the previous analysis to the MBE growth of group III nitrides, and clarify the thermodynamic characteristics of MBE growth.

The basic method of the present analysis is the same as that for group III arsenides, phosphides [5] and II–VI compounds [32]. The growth rate of MBE is controlled simply by the arrival rate or flux of group III or V atoms at the vapour–solid interface. The growth rate is expressed as follows:

$$r = k(P^0_{\mathrm{III}} - P_{\mathrm{III}}) \tag{28}$$

where $P^0_{\mathrm{III}} - P_{\mathrm{III}}$ indicates the driving force for the deposition, k is a constant, P^0_{III} is the

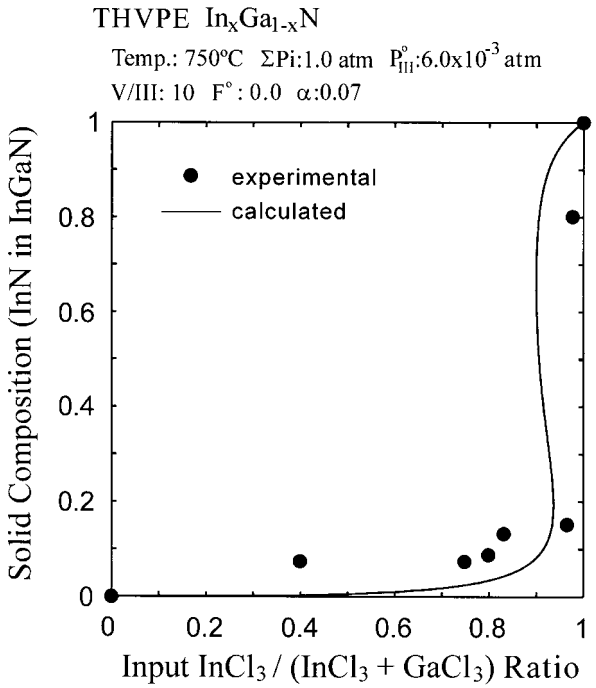

Figure 20. Comparison between the theoretically predicted and the experimental solid compositions of $In_xGa_{1-x}N$ alloys at 750 °C. The experimental data are taken from reference [31]. Total pressure: 1.0 atm; input partial pressure of group III sources: 6.0×10^{-3} atm; input V/III ratio: 10; F^0: 0.0; and α: 0.07.

pressure of the group III element incident on the substrate surface, and P_{III} is the equilibrium partial pressure at the vapour–solid interface. In this section, we analyse MBE growth systems using atomic nitrogen, which is generated by exciting nitrogen gas, and NH_3 gas as group V sources. As an example of the calculation procedure for MBE, we describe the epitaxial growth of GaN using atomic nitrogen. The chemical reaction which connects all species at the substrate surface is

$$\text{Ga (g)} + \text{N (g)} = \text{GaN (s)}. \tag{29}$$

The equilibrium equation for the reaction is as follows:

$$K_{29} = \frac{1}{P_{Ga} P_N}. \tag{30}$$

From the conservation constraint we have

$$P^0_{Ga} - P_{Ga} = P^0_N - P_N \tag{31}$$

where P^0_{Ga} and P^0_N are the input partial pressures which are obtained from the incident beam flux, and P_{Ga} and P_N are the equilibrium partial pressures. Equation (31) expresses the fact that the deposition occurs in the ratio of 1 to 1 for group III and group V elements.

The calculation for the MBE system using an NH_3 source was performed by a similar method to that used in the corresponding case using atomic nitrogen. The chemical reaction which connects species at the substrate surface is

$$\text{Ga (g)} + \text{NH}_3\text{ (g)} = \text{GaN (s)} + (3/2)\text{H}_2\text{ (g)}. \tag{32}$$

In this case, we introduce α, the mole fraction of decomposed NH_3, into the calculation as described in the section on MOVPE. The values of α in the following calculation are assumed appropriately as those for MOVPE growth, because it is difficult to know the exact value. Also, table 1 shows the equilibrium constants used in our calculation.

4.1. Binary group III nitrides

Figure 21 shows the equilibrium partial pressures over GaN as functions of the V/III ratio. As in group III arsenides and phosphides, a drastic change in partial pressure is seen at $V/III = 1$. When the V/III ratio is >1, the equilibrium partial pressure of Ga is very small, because of the deposition of Ga into the solid phase. On the other hand, for V/III < 1, the situation is reversed, and all N atoms are essentially incorporated into the solid. A similar relation is seen in the MBE system using the NH_3 source as shown in figure 22. In figure 22, partial pressures of H_2 and N_2 exist in addition to Ga and NH_3 in figure 21. In contrast to the case for MBE growth using atomic nitrogen, the position of the drastic change in partial pressure shifts to $V/III > 1$, due to the decomposition of NH_3.

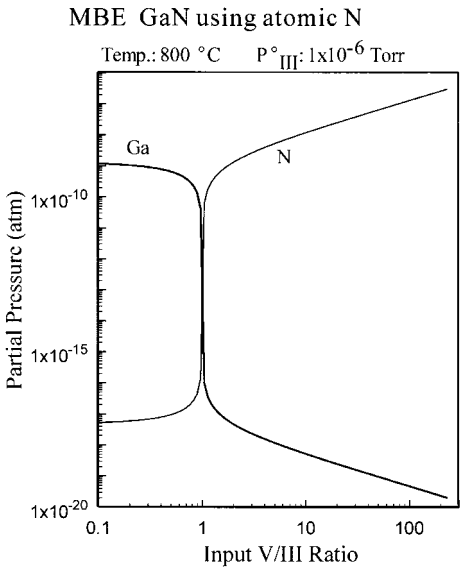

Figure 21. Equilibrium partial pressures over GaN as functions of input V/III ratio, using atomic nitrogen as the group V source.

In the MBE growth using atomic nitrogen, the growth rate depends on the input V/III ratio and the input partial pressure of the group III element. The driving force of the deposition increases with increase of the V/III ratio up to 1. Then, the growth rate becomes constant for $V/III > 1$. Also, the growth rate is a linear function of the input partial pressure of the group III element when the V/III ratio is >1.

Figure 23 shows, for GaN, InN and AlN, the normalized growth rate as a function of the growth temperature. The growth rate indicates the value of ΔP which is normalized to the low-temperature value. With increase of P^0_{III} or the input V/III ratio, the curves shift to the higher-temperature range. These facts show that the sublimation of InN, GaN and AlN is suppressed by the increase of P^0_{III} or the V/III ratio. From the figure we can predict the dependence of the growth rate on temperature as well as the sublimation temperature for

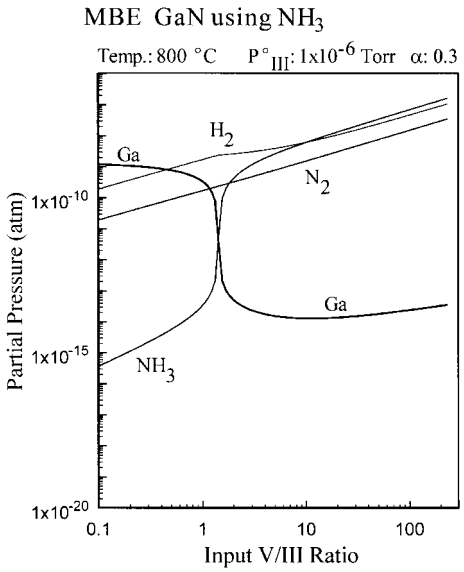

Figure 22. Equilibrium partial pressures over GaN as functions of input V/III ratio, using NH_3 as the group V source.

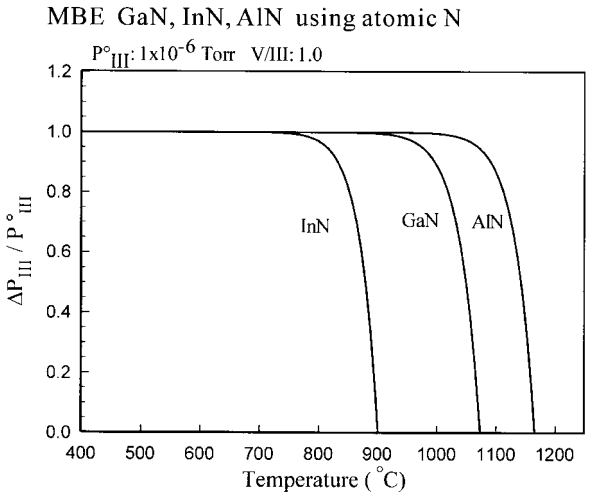

Figure 23. The normalized growth rates for GaN, InN and AlN as functions of growth temperature, using atomic nitrogen.

binary nitrides. For example, it is predicted that the growth rate of InN begins to decrease at about 740 °C, while that of AlN is independent of substrate temperature up to about 1140 °C. From figure 23, we have the following order for the sublimation of binary nitrides:

$$\text{AlN} > \text{GaN} > \text{InN}. \tag{33}$$

This order agrees with the order of the equilibrium constants for the following formation reaction of binary nitrides:

$$\text{III (g)} + \text{N (g)} = \text{III–N (s)}. \tag{34}$$

4.2. Ternary group III nitrides

Figure 24 shows ΔP $(=P^0_{\mathrm{III}} - P_{\mathrm{III}})$, i.e., the driving force for the deposition, as a function of solid composition, x in $In_xGa_{1-x}N$. In this calculation, the group V precursor was atomic nitrogen, and the input partial pressures of the group III sources and the input V/III ratio were kept constant at 1×10^{-6} Torr and 1.0, respectively. The driving force for the deposition strongly decreases with increase of the growth temperature over the whole solid composition range. However, this relation depends extremely strongly on the V/III ratio at the vapour–solid interface; that is, the driving force decreases with decreasing input V/III ratio especially in the high-temperature range and it is difficult to obtain InGaN alloys with low In concentrations for V/III < 1, as described later. Relations similar to those shown in figure 24 are obtained for the MBE system using an NH_3 source (not shown here).

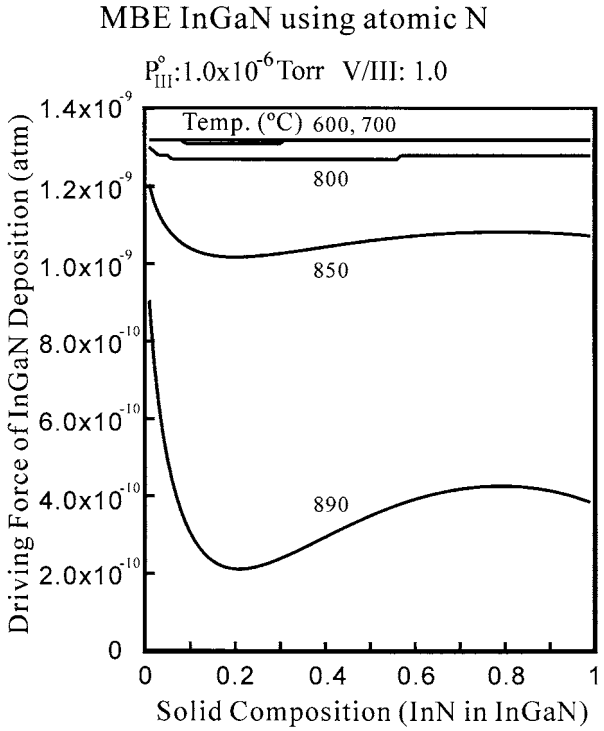

Figure 24. The driving force for the deposition as a function of the solid composition, x in $In_xGa_{1-x}N$, for several growth temperatures, using atomic nitrogen.

Figure 25 shows theoretical curves for the InGaN vapour–solid relation for several values of the V/III ratio. In the calculation, the growth temperature and the input partial pressures of the group III sources were kept constant at 800 °C and 1×10^{-6} Torr, respectively. The solid composition depends strongly on the input V/III ratio and a linear function of the vapour–solid distribution can be obtained at $V/III > 1$, i.e., the preferential incorporation of GaN is expected at small V/III ratios.

Theoretical curves for the InGaN vapour–solid relation for several growth temperatures are shown in figure 26. The solid composition deviates from a linear function with increasing growth temperature of the InGaN alloy. These relations are very similar to those for the MOVPE system. From this figure, it is seen that the iso-temperature line at 890 °C changes

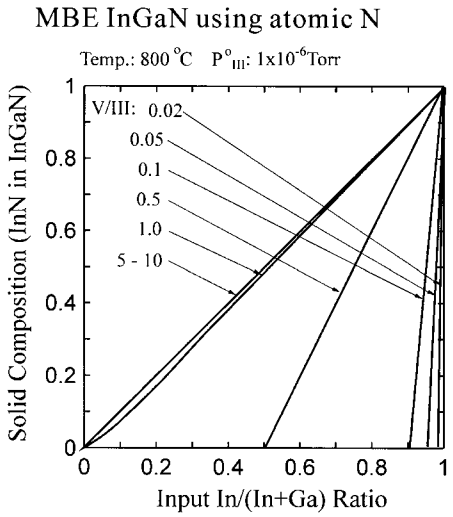

Figure 25. Theoretical curves showing the $In_xGa_{1-x}N$ solid composition as a function of the input mole ratio of the group III fluxes, for V/III ranging from 0.02 to 10.

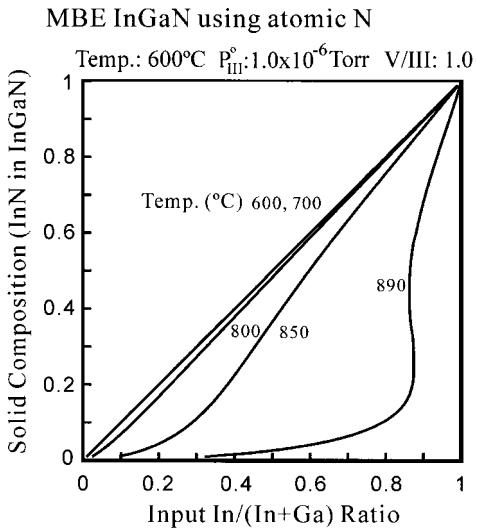

Figure 26. Theoretical curves showing the $In_xGa_{1-x}N$ solid composition as a function of the input mole ratio of the group III fluxes, for temperatures ranging from 600 to 890 °C.

in an inverse manner in the solid composition range from 0.2 to 0.5. This behaviour indicates that the deposition of compounds with various solid compositions is expected for a given input ratio of the group III fluxes. That is, it is shown that unstable regions, in which compounds with several compositions are formed for a given input mole ratio, exist in the alloy system. The unstable regions of solid composition will be discussed later. As described above, the relationship depends strongly on the input V/III ratio, and a drastic change in the vapour–solid relation occurs when growth conditions with V/III < 1 are used. On the basis of these results, it is found that the input V/III ratio is the most effective factor for controlling the solid composition in MBE.

5. The unstable region of solid composition for III nitride alloys

The growth of high-quality nitride alloys with large In contents is difficult, because of the unstable compositional nature of the alloy and the deposition of indium droplets. We have reported the thermodynamic characteristics of MOVPE [6, 33, 34], HVPE and MBE and the existence of an unstable region during the growth of InGaN. To grow high-In-content nitride alloys or films with homogeneous composition, it is necessary to obtain a detailed understanding of the unstable nature.

Figures 27 and 28 present theoretical curves showing the solid compositions of InGaN and InAlN grown by MOVPE as functions of the input mole ratio of the group III metal–organic sources for several growth temperatures. Although the solid composition of InAlN is a linear function of the input mole ratio at low growth temperature, the solid composition, for both alloys, deviates from a linear function with increasing growth temperature. One important feature in these figures is that the iso-temperature lines change in a complex manner at high temperatures. This indicates that the deposition of compounds with various solid compositions is expected for a given input mole ratio of the group III metal–organic sources. The unstable region of solid composition increases in magnitude with increasing growth temperature, and it appears more readily for the InAlN alloy. An unstable region also exists under conditions of high mole fraction of hydrogen and low V/III ratio.

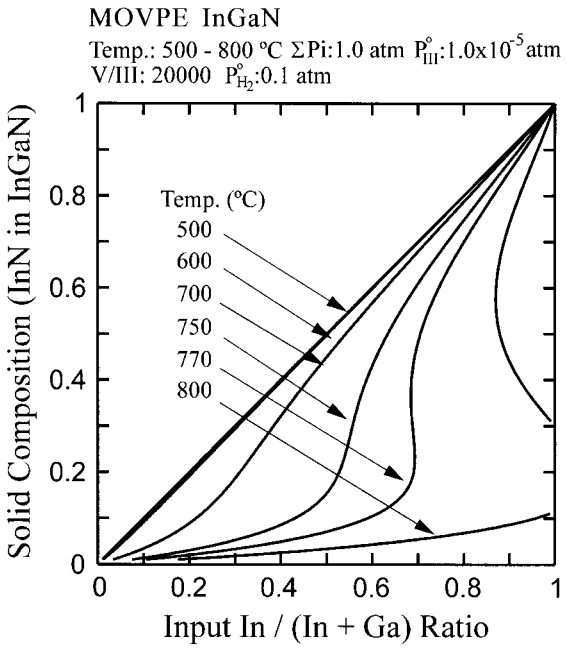

Figure 27. Theoretical curves showing the InGaN solid composition as a function of the input mole ratio of the group III metal–organic source, for temperatures ranging from 500 to 800 °C.

Figure 29 shows the growth efficiencies defined by $\Delta P_{\mathrm{In}}/P^0_{\mathrm{In}}$ and $\Delta P_{\mathrm{Ga}}/P^0_{\mathrm{Ga}}$ as functions of the solid composition in InGaN MOVPE at 790 °C. Since the equilibrium partial pressure of Ga is very low as shown in figure 7, the efficiency for Ga is almost unity over the entire composition range irrespective of temperature. In contrast to this, the efficiency for In is very small near $x = 0.2$ at 790 °C. These facts indicate that at high temperature, most of the input Ga deposits into the solid phase, whereas In remains in the vapour phase without deposition.

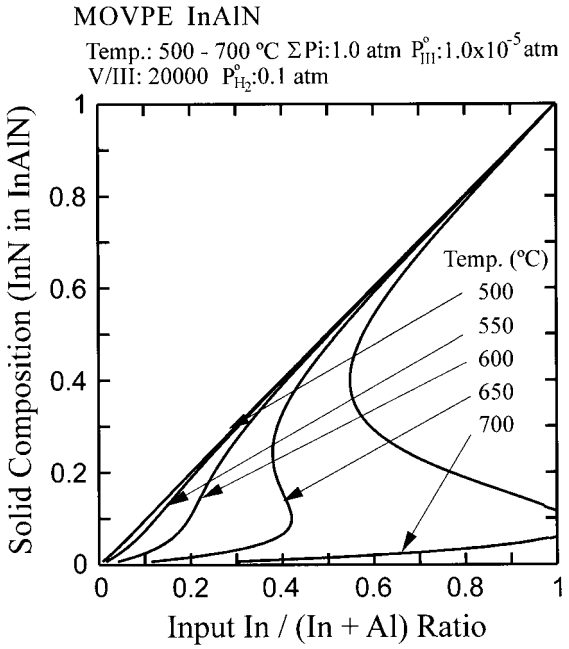

Figure 28. Theoretical curves showing the InAlN solid composition as a function of the input mole ratio of the group III metal–organic source, for temperatures ranging from 500 to 700 °C.

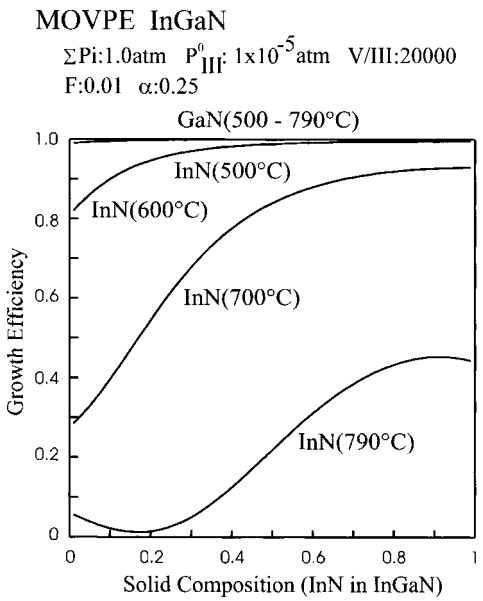

Figure 29. The growth efficiencies defined by $\Delta P_{\mathrm{In}}/P^{0}_{\mathrm{In}}$ and $\Delta P_{\mathrm{Ga}}/P^{0}_{\mathrm{Ga}}$ as functions of the solid composition.

Additionally, it can be seen that at high temperature the efficiency of In decreases with the increase of the solid composition up to 0.2; then it starts to increase, reflecting the relationship

between P_{In} and solid composition indicated in figure 7. It should be noted that the behaviour of $\Delta P_{In}/P^0_{In}$ and P_{In} causes unstable-composition (multi-composition) growth when the growth is performed at 790 °C or at low V/III ratio. From the calculation, it is found that the preferred growth conditions for high-In-content nitride alloys and/or epitaxial films with homogeneous composition are: use of higher input group III partial pressure, high V/III ratio and almost inert carrier gas.

6. A thermodynamic calculation system on the web

As described above, it is very important to know the mechanisms that determine the incorporation of elements in vapour-phase epitaxy such as MOVPE, HVPE and MBE. Thermodynamics provides us with very useful information, for example the driving force for the deposition and the vapour–solid distribution relation. Therefore, by using the equilibrium models prior to epitaxial growth, we can predict the growth rate and alloy composition under given growth conditions, or favourable growth conditions for compounds.

Equilibrium partial pressures in vapour-phase epitaxy, however, are significantly influenced by the growth conditions such as the kind of growth method and a lot of growth parameters. Accordingly, all crystal growers should have a thermodynamic calculation system to predict their crystal growth conditions. Such a system is quite difficult to establish, because the solution of equilibrium models generally involves many difficulties, such as a lot of growth parameters, a narrow convergent radius and a large number of iterations. Recently, we have constructed a thermodynamic calculation system on the Web for group III nitrides grown by MOVPE. The system consists of CGI scripts for information exchange, a main numerical calculation program and a graphic image generator for the user-friendly interface.

In the current system, thermodynamic analysis systems for the MOVPE growth of ternary group III nitrides such as InGaN, AlGaN and InAlN are available. Using an Internet browser, users can calculate equilibrium partial pressures thermodynamically under the growth conditions input by themselves, and also the vapour–solid distribution relation can be easily obtained. The URL for this system is http://epi.chem.tuat.ac.jp/; it is cost-free.

7. Conclusions

The element incorporation in group III nitride compounds grown from the vapour has been discussed. The driving forces for the deposition and the equilibrium partial pressures of group III nitrides grown by MOVPE, HVPE and MBE were thermodynamically analysed. It was found that the solid composition of epitaxial layers is basically governed by the Gibbs free energy of formation of binary compounds irrespective of the growth method. It was also shown that the growth under an almost inert carrier gas with higher input group III partial pressure and higher input V/III ratio is preferable for homogeneous nitrides and/or nitrides with In-rich content.

Acknowledgments

The authors would like to express their sincere thanks to Professor H Seki for his valuable suggestions on the thermodynamic analysis. Part of this work was supported by the JSPS Research for the Future programme in the area of Atomic Scale Surface and Interface Dynamics, No JSPS-RFTF97P00201.

References

[1] Koukitu A and Seki H 1980 *J. Cryst. Growth* **49** 325
[2] Stringfellow G B 1984 *J. Cryst. Growth* **70** 133
[3] Seki H and Koukitu A 1986 *J. Cryst. Growth* **74** 172
[4] Seki H and Koukitu A 1989 *J. Cryst. Growth* **98** 118
[5] Seki H and Koukitu A 1986 *J. Cryst. Growth* **78** 342
[6] Koukitu A, Takahashi N, Taki T and Seki H 1996 *Japan. J. Appl. Phys.* **35** L673
[7] Koukitu A, Takahashi N and Seki H 1997 *Japan. J. Appl. Phys.* **36** L1136
[8] Koukitu A, Takahashi N, Taki T and Seki H 1997 *J. Cryst. Growth* **170** 306
[9] Koukitu A and Seki H 1997 *Japan. J. Appl. Phys.* **36** L750
[10] Koukitu A, Kumagai Y and Seki H 2000 *J. Cryst. Growth* **221** 743
[11] Ban V S 1972 *J. Electrochem. Soc.* **119** 761
[12] Sedgwick T O and Smith J E Jr 1976 *J. Electrochem. Soc.* **123** 254
[13] Liu S S and Stevenson D A 1978 *J. Electrochem. Soc.* **125** 1161
[14] Stringfellow G B 1974 *J. Cryst. Growth* **27** 21
[15] Koukitu A and Seki H 1986 *J. Cryst. Growth* **76** 233
[16] Matsuoka T, Yoshimoto N, Sakai T and Katsui A 1992 *J. Electron. Mater.* **21** 157
[17] Matsuoka T, Tanaka H, Sakai T, Sasaki T and Katsui A 1989 *Gallium Arsenide and Related Compounds 1989 (Inst. Phys. Conf. Ser. 106)* (Bristol: Institute of Physics Publishing) p 141
[18] Matsuoka T, Yoshimoto, Sasaki T and Katsui A 1992 *J. Electron. Mater.* **21** 157
[19] McIntosh F G, Boutros K S, Roberts J C, Bedair S M, Piner E L and El-Masry N A 1996 *Appl. Phys. Lett.* **68** 40
[20] Matsuoka T 1997 *Appl. Phys. Lett.* **71** 105
[21] Dedair S M, McIntosh F G, Roberts J C, Piner E L, Boutros K S and El-Masry N A 1997 *J. Cryst. Growth* **178** 32
[22] Yamaguchi S, Kariya M, Nitta S, Kato H, Takeuchi T, Wetzel C, Amano H and Akasaki I 1998 *J. Cryst. Growth* **195** 309
[23] Maruska H P and Tietjen J J 1969 *Appl. Phys. Lett.* **15** 327
[24] Naniwae K, Itoh S, Amano H, Ito K, Hiramatsu K and Akasaki I 1990 *J. Cryst. Growth* **99** 381
[25] Motoki K, Okahisa T, Matsumoto N, Matsushima M, Kimura H, Kasai H, Takemoto K, Uematsu K, Hirano T, Nakayama M, Nakahata S, Ueno M, Hara D, Kumagai Y, Koukitu A and Seki H 2001 *Japan. J. Appl. Phys.* **40** L140
[26] Ban V S 1972 *J. Electrochem. Soc.* **119** 762
[27] Seki H and Minagawa S 1972 *Japan. J. Appl. Phys.* **11** 850
[28] Koukitu A and Seki H 1977 *Japan. J. Appl. Phys.* **16** 1967
[29] Takahashi N, Ogasawara J, Koukitu A and Seki H 1997 *J. Cryst. Growth* **172** 298
[30] Takahashi N, Matsumoto R, Koukitu A and Seki H 1997 *Japan. J. Appl. Phys.* **36** L743
[31] Takahashi N, Matsumoto R, Koukitu A and Seki H 1998 *J. Cryst. Growth* **198/190** 37
[32] Koukitu A, Nakai H, Suzuki T and Seki H 1987 *J. Cryst. Growth* **84** 425
[33] Koukitu A, Takahashi N, Taki T and Seki H 1997 *J. Cryst. Growth* **170** 206
[34] Koukitu A and Seki H 1996 *Japan. J. Appl. Phys.* **35** L1638
[35] Koukitu A, Hama S, Taki T and Seki H 1998 *Japan. J. Appl. Phys.* **37** 762
[36] Kumagai Y, Takemoto K, Koukitu A and Seki H 2001 *J. Cryst. Growth* **222** 118
[37] Kumagai Y, Takemoto K, Hasegawa T, Koukitu A and Seki H 2001 *J. Cryst. Growth* **231** 57